The effect of wind on the propagation rate of acoustic-gravity waves

By R. H. CLARKE, *C.S.I.R.O. Division of Meteorological Physics, Aspendale, Victoria, Australia*

(Manuscript received January 1, 1963, revised version September 19, 1963)

ABSTRACT

A method is described for deriving acoustic-gravity wave velocity in the presence of wind shear. It is used to calculate numerical weighting factors for a few special cases of two and three layer model atmospheres. These show that the wind velocity in a cold layer between two warm layers has a predominant positive influence on group velocity, and the wind at higher levels a negative influence, while phase velocity is quite differently affected.

The theory is illustrated by world-wide data relating to the Russian megaton explosion of 30 October 1961, and a study of global winds at the time. It was found possible to account for world-wide variations in wave propagation rate largely by a simple regression on the sine of the explosion longitude, which made possible estimates of effective wind over various ray path lengths. This was found, on the global scale, to be the mean of the wind in the 9–16 km layer, that is, approximately the mean wind in the "sound channel". Negative weightings at higher levels predicted by the model appear to be incorrect, and due to its inadequacy. The data strongly suggest that the "level of effective mean wind" is approximately that of the tropopause in middle latitudes.

Introduction

A number of workers have devoted themselves to describing and explaining the acoustic-gravity waves set up by large explosions, i.e. "aeroclysms" in the sense defined by SCORER (1958, p. 221). This author mentions that "Waves whose maximum amplitude is at the level of strongest wind will be propagated more rapidly than those whose maximum amplitude is at a level of light wind". WEXLER & HASS (1962), found good correlation between components of wind at 500 and 100 mb and propagation speeds of wave trains set up by the Russian megaton explosion of 30 October, 1961, in the west African, central Asian, central Pacific, central Atlantic and southern European areas. Elsewhere, "correlation was weak or negative". No other work on this subject is known, and it is desirable that it should be more thoroughly investigated.

We use the same nomenclature as Wexler and Hass, whereby the first wave train is designated A1, the second B1, the third A2, and so on, the time differential between A1 and A2, B1 and B2 being approximately 36 hours, the time taken to encompass the earth, and that between A1 and B1 36–2H, where H is the time lapse from the explosion to the arrival of the A1 train.

Since several oscillations of the A1 train from the explosion of 30 October 1961 were recorded by standard barographs over most of the world, and that of the B1, A2, B2, A3 were also recorded at a number of stations, these were examined in conjunction with global winds at the time to try to find empirical relationships. A theoretical investigation could also throw light on the problem if the dominant modes and frequencies of the large amplitude oscillations could be inferred. With regard to frequency, it is known that periods of the order of 5–12 minutes (DONN & EWING, 1962) dominate at the leading edge of the train. As to mode, HUNT, PALMER & PENNEY (1960) found a low frequency cut-off for the higher modes which exclude their consideration for periods of the order mentioned. This is supported by the much more detailed computations of PRESS & HARKRIDER (1962), who also concluded from a study of barograms that for long paths the higher modes are more attenuated than the fundamental, and that their so-called S_0 and GR_0

modes are sufficient to account for the first few oscillations of the B1 and A2 pulses. Hence we may confine our attention to the fundamental mode and periods of several minutes. We have not resorted to electronic computation, and thus for practical reasons are confined to consideration of two or three layer models. In principle, the method used can be extended to any number of layers, and the effect of wind in each of them determined. The empirical results provide a check on the general validity of our procedure.

Theoretical derivations of wave speeds, with wind included

We extend here the linearised theory developed by Scorer (1950), Hunt, Palmer & Penney (1960) and others, for the case of no wind shear, to include the case of a constant wind in each layer, confining our attention to vertical wave fronts propagating horizontally without change, and neglecting viscous dissipation. We use the system of the above-mentioned authors, in which the variable in the differential equation is $\tilde{\omega}$, given by

$$\tilde{\omega} + \tilde{\omega}_0 = \frac{\gamma R}{\gamma - 1}\left(\frac{p + p_0}{p_{0s}}\right)^{(\gamma-1)/\gamma}, \qquad (1)$$

where p_{0s} is a standard pressure, subscript 0 refers to unperturbed values, $\tilde{\omega}$, p are perturbation quantities, and γ, R, the standard gas constants for air.

At an interface between any two layers, the appropriate condition (Scorer, 1951; Press & Harkrider, 1962), neglecting higher order terms, is

$$p_1 - (\varrho_1 + \varrho_{01}) g\delta z = p_2 - (\varrho_2 + \varrho_{02}) g\delta z, \qquad (2)$$

where $p_1, p_2, \varrho_1, \varrho_2$ are respectively pressure and density perturbations on either side of the mean height of the interface, and δz the displacement of the interface from its equilibrium height h. Assuming sinusoidal perturbations of the interface and of w, the vertical velocity, we see that

$$\delta z = \int_0^t w\, dt = \frac{w}{i\sigma} \qquad (3)$$

and

$$\frac{w_1}{\sigma_1} = \frac{w_2}{\sigma_2}, \qquad (4)$$

where t is time, and σ_1, σ_2 respectively the frequencies in the layers *as noted by an observer moving with the wind.*

Since $U - v_1 = \sigma_1/k$, $U - v_2 = \sigma_2/k$, where U is the phase velocity relative to the ground, v_1, v_2 the wind speeds in the direction of wave propagation, and k the wave number, invariant with height,

$$\frac{w_1}{U - v_1} = \frac{w_2}{U - v_2}$$

which expresses the fact that the disturbed boundary represents a streamline in both systems.

Hunt, Palmer & Penney (1960) have shown (p. 280) from the equations of motion, that

$$w = \frac{i\sigma\tilde{\omega}'}{\sigma^2 \tau_0 + g\tau_0'}, \qquad (5)$$

where the prime indicates differentiation with respect to height, z, and the reciprocal of potential temperature,

$$\tau + \tau_0 = \frac{1}{T + T_0}\left(\frac{p + p_0}{p_{0s}}\right)^{(\gamma-1)/\gamma},$$

where $T + T_0$ is temperature. We note also that in an isothermal atmosphere

$$\tau_0'/\tau_0 = \frac{-(\gamma - 1) g}{c^2},$$

where g is gravity and c the speed of sound, given by $c^2 = \gamma R T$.

Using the relation $p = (\varrho_0/\tau_0)\tilde{\omega}$ and relations (2), (3), (4) and (5), we obtain the condition to be satisfied at each interface

$$\frac{1}{c_1^2}\left\{\frac{\tilde{\omega}_1}{\tilde{\omega}_1'}\beta_1 - g\right\} = \frac{1}{c_2^2}\left\{\frac{\tilde{\omega}_2}{\tilde{\omega}_2'}\beta_2 - g\right\}, \qquad (6)$$

where $$\beta_\alpha = \sigma_\alpha^2 - \frac{(\gamma - 1) g^2}{c_\alpha^2}.$$

We now employ (6) to derive equations $F_2(U) = 0$, $F_3(U) = 0$ respectively for two and three layer models, to be solved to obtain phase velocity U. Boundary conditions $w = 0$ at $z = 0$, and finite energy in a vertical column are imposed, as in Hunt, Palmer and Penney. Subscripts t, s are used for the two layer model for "troposphere" and "stratosphere", loosely applied, and t,s,u for the three layer model, u being the highest layer, extending to infinity.

Hunt, Palmer and Penney have given the general solution of the differential equation (their equation 25) for the case of a layer of constant temperature, as

$$\tilde{\omega} = C \exp \varkappa z + D \exp \lambda z.$$

The constants C and D must be so disposed that boundary conditions are satisfied, but the absolute amplitude of $\tilde{\omega}$ remains arbitrary. External boundary conditions are satisfied if in the highest layer

$$\tilde{\omega} = D \exp \lambda z \tag{7}$$

and in the lowest

$$\tilde{\omega} = E(-\lambda \exp \varkappa z + \varkappa \exp \lambda z) \tag{8}$$

while internal boundaries must satisfy (6).

In (7) and (8)

$$\varkappa_\alpha = P_\alpha + D_\alpha,$$

$$\lambda_\alpha = P_\alpha - D_\alpha,$$

$$P_\alpha = \frac{(2-\gamma) g}{2c_\alpha^2},$$

$$D_\alpha^2 = P_\alpha^2 - \beta_\alpha L_\alpha,$$

$$L_\alpha = \frac{1}{c_\alpha^2} - \frac{k^2}{\sigma_\alpha^2}.$$

Here D_α is a function of both phase velocity U and wind speed, v_α, in the direction of wave propagation, since σ_α is the frequency as noted by an observer moving with the wind.

For a two-layer model, (7) and (8) can easily be patched together by means of (6), by observing that in the upper layer

$$\frac{\tilde{\omega}}{\tilde{\omega}'} = \frac{1}{\lambda_s}$$

and in the lower

$$\frac{\tilde{\omega}}{\tilde{\omega}'} = \frac{-\lambda_t \exp \varkappa_t h_1 + \varkappa_t \exp \lambda_t h_1}{\lambda_t \varkappa_t (-\exp \varkappa_t h_1 + \exp \lambda_t h_1)}$$

which can be reduced to

$$\frac{\tilde{\omega}}{\tilde{\omega}'} = -\frac{S_t}{L_t \beta_t},$$

where $S_t = D_t \coth h_1 D_t - P_t$ and h_1 is the height of the interface. By substituting these expressions for $\tilde{\omega}/\tilde{\omega}'$ in (6) we obtain $F_2(U,a,b)$ where a,b are now written for v_1, v_2 the wind components:

$$F_2(U,a,b) = 0 = \delta_t(U,a) - \delta_s(U,b) \tag{9}$$

writing
$$-\frac{1}{c_t^2}\left(\frac{S_t}{L_t} + g\right) = \delta_t$$

and
$$\frac{1}{c_s^2}\left(\frac{\beta_s}{\lambda_s} - g\right) = \delta_s.$$

The derivation of $F(U,a,b,c)$ is tedious, but straightforward and along similar lines, and results in:

$$\begin{aligned} F_3(U,a,b,c) = 0 = {} & \varkappa_s(U,b) X(U,a,b,c) \\ & + \lambda_s(U,b) Y(U,a,b,c) \\ & - \beta_s(U,b) \\ & - L_s(U,b)\,\Delta_t(U,a)\,\Delta_u(U,c), \end{aligned} \tag{10}$$

where a,b,c are wind components in the lowest, middle and highest layer respectively,

$$X = \frac{\Delta_u \exp N - \Delta_t \exp(-N)}{2 \sin hN},$$

$$Y = \frac{\Delta_t \exp N - \Delta_u \exp(-N)}{2 \sin hN},$$

$$\Delta_t = c_s^2 \delta_t + g,$$

$$\Delta_u = \frac{c_s^2}{c_u^2}\left(\frac{\beta_u}{\lambda_u} - g\right) + g,$$

$$N = (h_2 - h_1) D_s,$$

h_1, h_2 = height of lower (or only) and upper interface, respectively.

It can be shown that (9) reduces to the equation for gravity waves in a two layer model (SCORER, 1951; GOSSARD & MUNK, 1954; CLARKE, 1962) when U is small compared with the velocity of sound: i.e. in addition to solutions corresponding to acoustic-gravity waves with velocities comparable with that of sound, there is another class corresponding to what have been called "Helmholtz waves", varying in phase velocity from zero upwards, depending

TABLE 1. *Computed weighting factors for the effect of wind on wave velocity in two- and three-layer models.*

No. of layers	2	2	2	2	2	2	3
Height of lower interface (h_1, km)	9.61	15.85	40	40	40	40	10
Height of upper interface (h_2)	—	—	—	—	—	—	20
T_t (tropospheric temp.) °C	258	252.2	250	250	250	250	260
T_s (stratospheric temp.) °C	229.3	200	320	320	320	320	220
T_u (upper layer temp.) °C	—	—	—	—	—	—	250
Mode (no. of nodes)	0	0	0	0	0	1	0
Wave-length (km)	80	80	80	150	12	12	80
Phase velocity (m sec^{-1})	311.65	307.00	320.93	323.22	317.51	323.87	313.71
Group velocity	311.03	303.28	317.64	319.78	317.09	311.74	313.05
Weighting factors							
Phase velocity							
Troposphere ($\partial U/\partial a$)	0.464	0.610	0.854	0.790	0.998	0.984	0.455
Stratosphere ($\partial U/\partial b$)	0.536	0.290	0.146	0.210	0.002	0.016	0.247
Upper layer ($\partial U/\partial c$)	—	—	—	—	—	—	0.298
Group velocity							
Troposphere ($\partial c_g/\partial a$)	0.376	0.283	1.778	1.379	2.785	2.606	0.387
Stratosphere ($\partial c_g/\partial b$)	0.624	0.717	−0.778	−0.379	−1.785	−1.606	1.043
Upper layer ($\partial c_g/\partial c$)	—	—	—	—	—	—	−0.430

on gravity and shear, but not on compressibility.[1]

We have been content to calculate weighting factors for the wind in the two- and three-layer models, describing the effect of the wind in each of these layers on both phase and group velocity. The weighting factors are respectively $\partial U/\partial a$, $\partial U/\partial b$, $\partial U/\partial c$ for the phase velocity, and (writing $c_g = U + k\, \partial U/\partial k$ for group velocity), $\partial c_g/\partial a$, $\partial c_g/\partial b$, $\partial c_g/\partial c$ for group velocity. The phase velocity, given the weighting factors, can then be calculated from the expression

$$U = U_0 + a\frac{\partial U}{\partial a} + b\frac{\partial U}{\partial b} + c\frac{\partial U}{\partial c}$$

provided a,b,c are small enough, where U_0 is the phase velocity with no wind. A similar expression applies for c_g.

These weighting factors have been computed by partial differentiation of F with respect to U,a,b,c,k (at $a=b=c=0$), employing such identities as

$$-\partial U/\partial a = \partial F/\partial_a\,(\partial F/\partial U)^{-1},$$

$$c_g = U + k\,\partial U/\partial k = U - k\,\partial F/\partial k\,(\partial F/\partial U)^{-1}.$$

Table 1 sets out the result of these computations.

The two-layer models chosen were those treated by Hunt, Palmer and Penney, while the three-layer model was chosen after an examination of world temperatures and winds (MURGATROYD, 1957), in an attempt to obtain the most representative divisions with regard to both, up to 30 km.

It appears that, so far as these models can tell us, the group velocity is affected by wind in a manner quite different from phase velocity. The latter appears to be influenced by the mass in the layers, while the former appears to be very sensitive to the wind in the cold layer, which is strongly positively weighted, while a warm upper layer is negatively weighted. It is possible that these features would not occur in a more adequate model, but heavy weighting in the sound channel appears to be borne out by evidence presented below.

The variation of weighting factors with wave-length suggests that dispersion should be strongly affected by a height-variant wind structure, so that inverse dispersion (group velocity decreasing with wave-length) might occur. It is more probable that a two-layer model cannot be relied on to give even qualitatively correct answers concerning dispersion effects of wind in the real atmosphere.

From the one case investigated, it would seem that the mode with one node in the vertical differs but little in its weighting characteristics from the fundamental.

[1] Equations (9) and (10), reduced to their no-shear form ($a=b=c$) differ from corresponding equations derived by HUNT, PALMER & PENNEY (1960, equations 37,47) which are evidently incorrect, as has been noted by PRESS & HARKRIDER (1962, p. 3890).

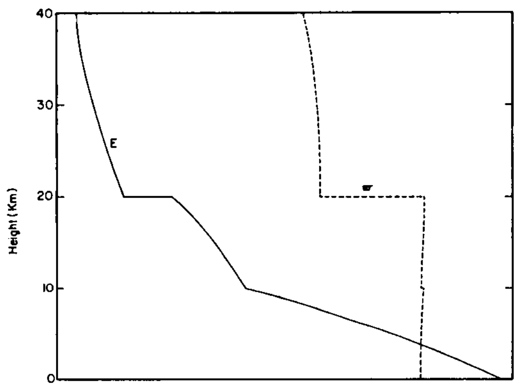

FIG. 1. Vertical distribution of amplitude of energy transmission E, and modified pressure $\tilde{\omega}$, computed for a three-layer model.

In order to compare the effect of temperature in the three-layer model with that of wind, for the fundamental mode, weighting factors for c_t, c_s, c_u were computed in the same way as for a, b, c putting $a = b = c = 0$, and varying the c's in turn. The result (for wave-length 80 km only) indicates that the effect of varying these was closely similar on both the phase and group velocities; these varied in each case in the same sense as temperature, the weighting factors being

$$\frac{\partial U}{\partial c_t} = 0.454, \quad \frac{\partial U}{\partial c_s} = 0.238, \quad \frac{\partial U}{\partial c_u} = 0.308.$$

Having found a solution for U from (10), we can compute the vertical distribution of $\tilde{\omega}$ in arbitrary units (fundamental mode, no wind shear), by solving for A, B, C in the equations governing this distribution:

$$\tilde{\omega}_u = A \exp \lambda_u z \exp i\sigma t,$$

$$\tilde{\omega}_s = B(\exp \varkappa_s z + \exp \lambda_s z) \exp i\sigma t,$$

$$\tilde{\omega}_t = C(-\lambda_t \exp \varkappa_t z + \varkappa_t \exp \lambda_t z) \exp i\sigma t$$

and thereby obtain the vertical distribution of $\tilde{\omega}, w, p, u$ (the horizontal wind perturbation) and $E \propto up$, the energy transmission.

$$E = \tilde{\omega}^2 T_0 p_0^{(2-\gamma)/\gamma}.$$

In Fig. 1 are represented the vertical distribution of $\tilde{\omega}$ and E, the former having almost constant amplitude up to h_2, the latter diminishing rather rapidly with height. This figure differs considerably from corresponding figures by Hunt, Palmer and Penney, where the discontinuities at h_1, h_2 do not appear through their erroneous interface conditions.

The bending effect of zonal wind and meridional temperature gradients on rays emanating from an explosion

A ray, which gives the direction and speed of energy propagation, emanating from an explosion, is refracted by both temperature and wind inhomogeneities.

The zonal wind may be used to compute refraction on the global scale, if we know the "effective level" of the wind for this purpose. The wind at 200 mb should provide an upper limit for this effect, and this has been used in the ray tracing which follows (Fig. 2a and b).

MULLALY (1962) has shown that the curvature K of a ray of a plane wave in a medium with wind, but otherwise uniform, is given by[1]

$$K = WK_w - \frac{1}{c_g} \cos \mu \frac{\partial w}{\partial x_T},$$

where $W = w/c_g$, w is wind velocity, c_g is velocity of the wave in a stationary medium, K_w is curvature of the wind streamline, μ is the angle between the wind and the ray, and x_T is distance perpendicular to the ray.

The wave in this case is not plane, but we can project the ray on to a tangent plane and plot its course. In this case, for a zonal wind, $K_w = (1/a) \cot \varphi$, where a is the earth's radius, and φ the angular distance from the north pole.

The curves in Fig. 2 were obtained by integrating the equation

$$ac_g K = u_{200} \cot \varphi - \cos^2 (\alpha - \psi) \frac{du_{200}}{d\varphi},$$

u_{200} being mean zonal wind at 200 mb, c_g 310 m sec^{-1}, α the angle between zonal wind and original explosion meridian of a ray, ψ that between the ray and this meridian. The explosion longitude λ' of a point on the earth is defined as the angle between the great circle through north pole and explosion site and that joining the point to the explosion site, and is positive if anticlockwise. The other explosion co-ordinate, φ', is angular distance from the explosion. The rays traced in Figure 2 are those

[1] The sign of the first term on the right-hand side has been changed, with the concurrence of the author.

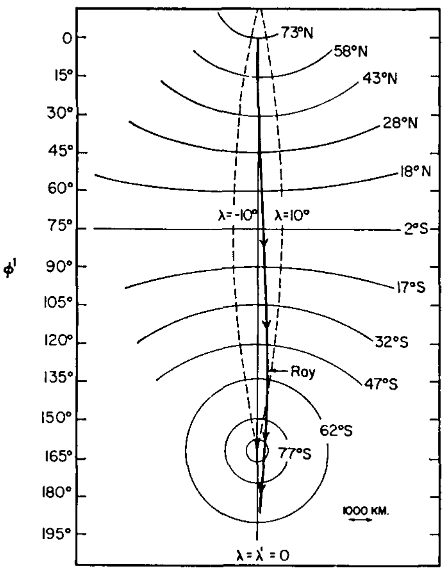

(a)

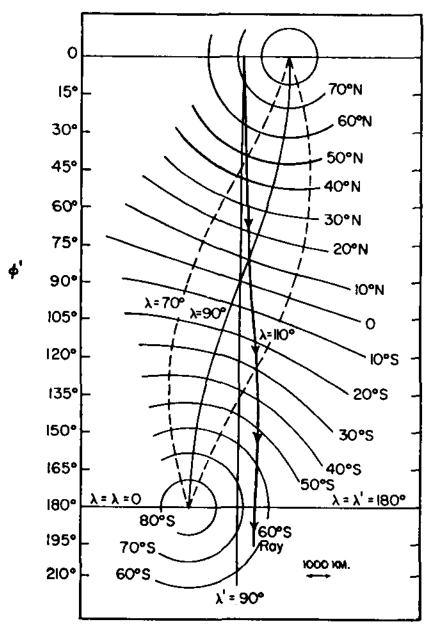

(b)

FIG. 2. The path of a ray, refracted by wind at 200 mb, setting out on an explosion longitude of (a) $\lambda' = 0$, (b) $\lambda' = \frac{1}{2}\pi$, projected on to a cylinder touching the globe along the great circles (a) $\lambda' = 0$ and (b) $\lambda' = \frac{1}{2}\pi$.

starting from the explosion at explosion longitudes 0 and $\frac{1}{2}\pi$. It is seen that the ray departs, by the time it reaches the explosion antipode, by respectively about 100 and 900 km from the great circle on which it commenced, and that the error in assuming that it follows a great circle path is nowhere great. On its return journey from the antipode, it will be refracted to approximately the same extent, so that the path followed will be nearly the same on each circuit of the earth, in so far as it is affected by zonal winds.

PRESS & HARKRIDER (1962) have shown by computation that the variation in group velocity from an arctic winter to a tropical atmosphere for the wave-lengths of interest should be from 302 to 315 m $\sec^{-1}$, and we should therefore expect refraction due to temperature gradients. In an attempt to estimate this quantitatively, it was assumed that the only effect on group velocity arises from the layer 1000 − 300 mb, where the weighting factor $\partial c_g/\partial c_t = 0.45$ found for the three layer model t was assumed to apply. The variation of c_t with latitude was obtained from the global mean 1000 − 300 mb thickness distribution, available from the wind studies. Refraction of the ray starting on an explosion meridian of $\lambda' = \frac{1}{2}\pi$ was calculated, assuming no wind, by integrating the relation

$$K = -\frac{1}{c_g}\frac{dc_g}{dx_T} = -\frac{.45}{c_g}\cos(\alpha - \psi)\frac{d\sqrt{\gamma R T_m}}{d\varphi},$$

where $$T_m = \frac{g\Delta Z}{R\ln(1000/300)}$$

and ΔZ is the thickness. This computation yielded the result that the deviating effect of temperature gradient on the global scale is only about one-eighth that of the wind, for $\lambda' = \frac{1}{2}\pi$, and is of course nil for $\lambda' = 0, \pi$.

In view of the foregoing, it should be expected that on the global scale, the main factor in determining departure of mean speed of propagation from normal, when mean speeds are measured by shortest circumferential distance divided by time, will be the extent to which the ray is assisted by the component of zonal wind in the direction of propagation. Temperature effects on forward speeds for long paths are expected to be fairly similar on all rays, thanks to the high latitude of the explosion. The observations enable us to test this argument.

TABLE 2. *Details of the regression of propagation velocity on the sine of the explosion longitude, the deduced mean effective zonal angular velocity of the wind, and the mean value of φ_R' for each group of observing stations.*

Category	Description	No. of obs. (n)	e (m sec^{-1})	f (m sec^{-1})	Proportion of variance (ϱ)	Effective angular velocity $\times 10^6$ (radians sec^{-1}) $q=17°$	$q=15°$	Mean φ_R' (degrees)
(*a*)	A1, N.H.	133	309.48	8.30	0.253	$\dot{\lambda}_a$ 4.46	5.03	50.6
(*b*)	A1, S.H.	103	310.75	4.95	0.396	$\dot{\lambda}_b$ 2.66	3.01	124.6
(*c*)	All A1	236	310.12	6.17	0.273	$\dot{\lambda}_c$ 3.31	3.74	83.0
(*d*)	B1, N.H.	23	310.24	6.03	0.798	$\dot{\lambda}_d$ 3.24	3.66	320.7
(*e*)	B1, S.H.	57	309.56	6.68	0.581	$\dot{\lambda}_e$ 3.59	4.05	233.7
(*f*)	All B1	80	309.96	6.39	0.708	$\dot{\lambda}_f$ 3.43	3.87	258.7
(*g*)	A1, B1 south of 35° S	58	310.67	5.96	0.736	$\dot{\lambda}_g$ 3.20	3.61	173.1
(*h*)	A2, A3, B2	34	310.12	6.27	0.831	$\dot{\lambda}_h$ 3.37	3.81	360

Effective zonal wind derived from a world network of barograms

In a φ,λ system based on the north pole, we assume a zonal wind of angular velocity $\dot{\lambda}$, and find, by simple spherical trigonometry, that in the φ',λ' system based on the explosion site, the component of angular velocity in the explosion meridional direction is given by

$$\dot{\varphi}' = \dot{\lambda}\sin q \sin\lambda', \qquad (11)$$

where q is the colatitude of the explosion, while

$$\dot{\lambda}' = \dot{\lambda}(\cos q + \sin q \cot\varphi' \cos\lambda') \qquad (12)$$

is the zonal angular velocity in explosion co-ordinates. From the spherical triangle we also obtain the relation

$$\sin\lambda' = \frac{\sin\lambda \sin\varphi}{\sin\varphi'}.$$

From (11), we expect the mean velocity of the wave arriving at any point whose explosion co-ordinates are (φ',λ') and whose north polar co-ordinates are (φ,λ) to be augmented by an amount given approximately by

$$\Delta c_g = a\,\dot{\lambda}\sin q \sin\lambda' \qquad (13)$$

where $\dot{\lambda}$ is now the mean angular velocity of zonal wind over the path of the ray, and λ', as we have seen, is sensibly constant over the path.

This is checked by means of a world-wide network of observations of V, the measured mean speed of the wave train. (Strictly the great circle distance of the observing point from 73° N, 55° E, divided by elapsed time from 0833 G.M.T. on 30 October, 1961 to the time of the first barograph displacement, for A1, B1 waves, and the circumference of the earth divided by elapsed time from the A1 to A2 or B1 to B2 passages for A2, B2 waves.)

The observations, taken from individual barograms, have been supplied by a number of organisations and individuals, listed under "Acknowledgements". They include all barograms showing the oscillations from the following countries (with the number of observing stations in brackets): Australia and New Guinea (33), Japan (10), New Zealand (14), Antarctica (6), Argentine (34), South Africa (15), Equatorial Africa (3), Canada (41), India (40), Pakistan (7), Singapore (1), the Pacific Islands (11) and some from the United States (12). In addition, published material from Great Britain (JONES, 1962; ROSE, OKSMAN & KATAJA; 1961) Austria (TOPERCZER, 1962), Sweden (ARASKOG, ERICSSON, ERICSSON & WÄGNER, 1962) and other places (DONN & EWING 1962; TANDON 1962) has been used, and a few others have been obtained by private correspondence. The total number of observations of at least one passage is 242.

We assume a regression $V = e + fx$, where $x = \sin\lambda'$, and find e,f,P, by standard procedures where $P = f^2$ (var x/var V) is the proportion of the variance of V accounted for by the regression. Values of e,f,P, for (*a*) all A1 pulses reported in the northern hemisphere, (*b*) A1 pulses reported in the southern hemisphere, (*c*) all A1 pulses, (*d*) B1 pulses in the northern hemisphere, (*e*) B1 pulses in the southern hemisphere, (*f*) all B1 pulses, (*g*) all A1 and B1 pulses south of 35° S, and (*h*) all A2, A3, B2 pulses, together with n, the number of observations and mean φ'_R, the angular distance covered by the ray reaching each station, are shown in Table 2.

The high values of P for the longer paths (B1, A2, etc.) indicate clearly that zonal winds are the preponderant influence on speed anomaly, while for shorter paths, timing errors, temperature and terrain effects, non-zonal winds and incorrect locating of the explosion site and time probably all contribute more significantly to the variance. This is reflected in the A1 data for northern latitudes, which show a wide scatter.

The value e represents mean velocity for $\lambda' = 0, \pi$, where zonal wind effects are nearly absent, and is probably close to the still air group velocity, averaged over the earth in the case of line (*h*).

The computations were made on the basis of an early estimate of 73° N, 55° E for the explosion site. Since then, published estimates have appeared giving the latitude as 75° N. A check calculation on southern hemisphere data showed that values of f obtained from the regression for longer path lengths are insensitive to the assumed latitude within this range. The value of f can be equated to a $\dot{\lambda} \sin q$ in equation (13), to give an estimate of $\dot{\lambda}_a, \dot{\lambda}_b \ldots$, the mean effective zonal angular wind velocity for the paths corresponding to the various groups of observations. These estimates are sensitive to the assumed latitude of the explosion, or q, the colatitude, and in Table 2, two values of $\dot{\lambda}_a, \dot{\lambda}_b \ldots$ are presented, based respectively on $q = 17°$ and $q = 15°$.

A survey of the global winds on 30–31 October 1961, and comparison with effective mean winds

Data used for the global wind survey were "Northern Hemisphere Data Tabulations" for 30 October 1961, published by the U.S. Weather Bureau; and aerological data for India, Australia, New Zealand and dependent islands, and Antarctica.

Northern hemisphere winds were obtained by plotting all available height data for each standard pressure level up to 10 mb, and averaging contour heights around circles of latitude. These were converted to winds by means of the geostrophic relation. Observed winds were used within 15° of the equator on either side. Southern hemisphere data are of course scanty, and in order to obtain from the limited coverage a more hemispherically representative zonal wind distribution, the 21 days' standard pressure heights up to 15 mb, centred on 31 October 1961, were averaged for each station. Thus the world distribution of zonal angular velocity was estimated for heights up to nearly 30 km, and areally meaned.

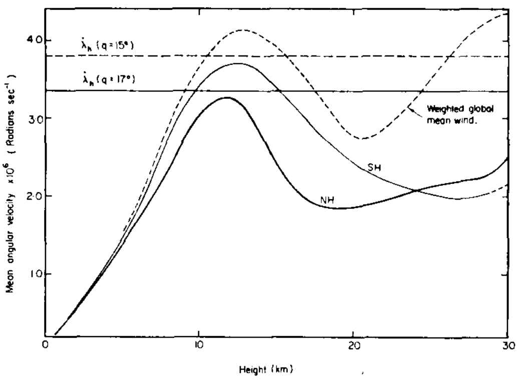

Fig. 3. Observed angular velocity of the global wind areally meaned (full curves), and weighted for a $\lambda' = \frac{1}{2}\pi$ ray (broken curve), compared with deduced effective mean global wind on the assumption of $q = 17°$ (full straight line) and of $q = 15°$ (broken straight line).

The result for each hemisphere is depicted by the full lines in Fig. 3, where the two values of $\dot{\lambda}_h$, the effective mean global angular velocity from Table 2, are shown as horizontal lines. This exceeds the *areal* mean of observed angular velocity at all levels, except possibly in the neighbourhood of 200 mb. However, rays from the explosion will experience a differently weighted mean. The effective weighting will probably lie between that for a ray on a course $\lambda' = 0$ and for one of $\lambda' = \frac{1}{2}\pi$. As far as can be judged, there is little difference in the global wind means for these two rays. The $\lambda' = \frac{1}{2}\pi$ ray was selected for treatment for the practical reason that very high latitude winds are inadequately known, and this ray avoids latitudes 90 to 73.

Progressive mean angular wind velocities were computed by time averaging (assuming

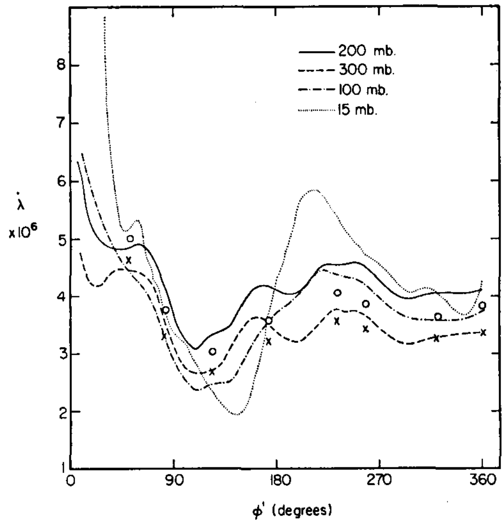

FIG. 4, Observed mean angular wind velocity $\dot{\lambda}$, weighted for a $\lambda' = \frac{1}{2}\pi$ ray, as a function of path length φ_R', at four levels, compared with effective mean wind, on the assumption of $q = 17°$ (crosses) and $q = 15°$ (circles).

a constant wave velocity) along this explosion longitude from $\varphi_R' = 0$ to $\varphi_R' = 2\pi$. The distribution of global means (i.e. $\varphi_R' = 2\pi$) with altitude is shown in Figure 3, by the broken line. It will be noted that $\dot{\lambda}_h$ is the average velocity approximately in the layer from 9 to 16 km (accepting $q = 15°$), but that this value is again exceeded at higher levels, due to the strong high latitude westerlies in both hemispheres.

It can hardly be expected that an effective wind computed from the weighting factors presented in Table 1 for a three-layer model should bear close comparison with the observations, because of the unreality of the model. In reality, the lower "sound channel" lies roughly between 9 and 16 km over most of the earth. The model suggests that the mean wind in this layer should be approximately the effective wind for wave propagation, and this is seen to be so from Fig. 3. The question of negative weighting at higher levels cannot be answered with available data, but a check at 5 mb of the scanty information at hand strongly suggests that weighted values of $\dot{\lambda}$ will increase with height above 30 km owing to the strong polar westerlies. It thus appears that the marked negative weighting factors computed are due to the artifices of the model, and that in the real atmosphere they are quite small above 30 km.

Weighting factors on a more refined scale cannot be computed without much effort, but it is possible to use $\dot{\lambda}_a, \dot{\lambda}_b$..... to deduce the "level of effective mean wind" in some detail. In Fig. 4, $\dot{\lambda}_a, \dot{\lambda}_b$... are represented by crosses ($q = 17°$) and circles ($q = 15°$), the abscissa being mean path length (φ_R') of the group of stations concerned, the ordinate, $\dot{\lambda}$ for various levels from 300 mb to 15 mb, calculated as functions of φ_R' from the mean zonal angular velocity of the observed wind for a $\lambda' = \frac{1}{2}\pi$ ray. Accepting $q = 15°$ as the correct colatitude of the explosion, one is surprised, in view of the defects of the method, at the fidelity with which all points except $\dot{\lambda}_a$ lie between the curves for 300 mb and 200 mb (or near 300 mb if $q = 17°$ is accepted), suggesting that the "level of effective mean wind" is close to that of the mid-latitude tropopause.

Conclusions

We are thus able to conclude that the crude three-layer model indicates the cold layer (in the model the layer 10–20 km, in the real atmosphere roughly 9–15 km) as the seat of the effective mean wind. A more refined model, with many layers, would be required to give a more precise answer to questions concerning the effect of wind on wave propagation. Such a procedure could also be used to find the effect of wind on dispersion.

The observations, used in the manner described, broadly support the theoretical findings, but suggest that the heaviest weighting factors for the wind should lie near 10 km rather than higher; it is the winds in the vicinity of the mid-latitude tropopause which largely determine the effect of wind on the propagation rate of the "aeroclysm". Wind weightings based on the energy transmission curve of Fig. 1 give erroneously low values for the effect of wind.

Acknowledgements

Most of the wave data have come from the national meteorological services of the countries mentioned, and their help is gratefully acknowledged. Special thanks are due to the following people for their active assistance: Mr. J. J. Taljaard of South Africa; Mr. W. A. Hass of the United States; Dr. D. Stranz of Kenya; Captain G. H. Gilbert of Canada; Drs. K.

Wölcken and J. A. J. Hoffmann of Argentine; Dr. J. F. Gabites of New Zealand; Mr. M. U. Khan of Pakistan; Dr. M. Båth of Sweden; Mr. C. E. Wallington of England; Dr. G. Stilke of Germany; Mr. N. Murayama of Japan; Dr. U. Radok, who obtained copies of Antarctic barograms; Messrs. W. J. Gibbs and H. R. Philpott of Australia. Finally, thanks are due to Mr. J. Wren, whose expert use of a desk computer made the computations practicable.

REFERENCES

ARASKOG, R., ERICSSON, U., and WÄGNER, H., 1962, Long-range transmission of atmospheric disturbances. *Nature*, **193**, pp. 970–1.

CLARKE, R. H., 1962, Pressure oscillations and fall-out downdraughts. *Quart. J. Roy. Met. Soc.*, 88, pp. 459–469.

DONN, W. L., and EWING, M., 1962, Atmospheric waves from nuclear explosions. *J. Geoph. Res.*, **67**, pp. 1855–1866.

DONN, W. L., and EWING, M., 1962, Atmospheric waves from nuclear explosions II. *J. Atmos. Sci.*, **19**, pp. 264–273.

FARKAS, E., 1962, Transit of pressure waves through New Zealand from the Soviet 50 megaton bomb explosion. *Nature*, **193**, pp. 765–6.

GOSSARD, E., and MUNK, W., 1954, On gravity waves in the atmosphere. *J. Meterology*, **11**, pp. 259–269.

HUNT, J. N., PALMER, R., and Sir WILLIAM PENNEY, 1960, Atmospheric waves caused by large explosions. *Phil. Trans. Roy. Soc. London*, Ser. A, No. 1011, **252**, pp. 275–315.

JONES, R. V., 1962, Subacoustic waves from large explosions. *Nature*. **193**, pp. 229–232.

MULLALY, R. F., 1962, Ray paths in inhomogeneous anisotropic media. *Aust. J. Physics* **15**, pp. 96–105.

MURGATROYD, R. J., 1957, Winds and temperatures between 20 km and 100 km—a review. *Quart. J. Roy. Met. Soc.*, **83**, p. 417–455.

PRESS, F., and HARKRIDER, D., 1962, Propagation of acoustic-gravity waves in the atmosphere. *J. Geophys. Res.*, **67**, pp. 3889–3908.

ROSE, G., OKSMAN, J., and KATAJA, E., 1961, Round the world sound waves produced by the nuclear explosion on October 30, 1961, and their effect on the atmosphere at Sodankylä. *Nature*, **192**, pp. 1173–1174.

SCORER, R. S., 1950, The dispersion of a pressure pulse in the atmosphere. *Proc. Roy. Soc. A*, **201**, pp. 137–157.

SCORER, R. S., 1951, Gravity waves in the atmosphere. *Archiv. Met. Geophys. Biokl. A*, **4**, pp. 176–193.

SCORER, R. S., 1958, *Natural Aerodynamics*, London, Pergamon Press, 312 pp.

TANDON, A. N., 1961, Seismic recording at Delhi of the Russian nuclear explosions on 23 and 30 October 1961, *Indian J. Met. and Geophys.*, **12**, pp. 604–608.

TOPERCZER, M., 1962, Atombombenexplosion und Luftdruckwellen. *Wetter und Leben*, **14**, pp. 1–6.

WEXLER, H., and HASS, W. A., 1962, Global atmospheric pressure effects of the October 30 1961 explosion. *J. Geophys. Res.* **67**, pp. 3875–3887.